كلية الهندسة بشبرا
FACULTY OF ENGINEERING AT SHOUBRA
ERJ
PRINT ISSN 3009-6049
ONLINE ISSN 3009-6022

ENGINEERING RESEARCH JOURNAL (ERJ)
Volume (53),Issue (2)
April 2024, pp:110-118
https://erjsh.journals.ekb.eg

Nonlinear Finite Element Modeling of Wooden Elements Strengthened by FRP

Ashwaq M. Osman [1,*], M.A.Aboshok [1], Gehan A. Hamdy [1], Osama O. El-Mahdy [1]

[1] *Civil Engineering Department, Faculty of Engineering at Shoubra, Benha University, Cairo, Egypt*
**Corresponding author*

E-mail address: ashwaq.osman19@feng.bu.edu.eg , Mohamed.aboshok@feng.bu.edu.eg , gehan.hamdy@feng.bu.edu.eg , osama.alhenawy@feng.bu.edu.eg

Abstract: Wooden beams have been traditionally used for centuries as the supporting elements for roofs. Long exposure to environmental conditions and aging cause deterioration and decay of the wooden beams in historical structures, whereby restoration or strengthening is often needed to preserve its historical and archaeological value. This research addresses wooden beams strengthened using Fiber-Reinforceded Polymers (FRP). Numerical modelling is carried out by Finite Element Method (FEM) using a commercial Simulia ABAQUS software ABAQUS, taking into account the anisotropic nature of wood materials and nonlinear behaviour. Validation of the numerical modelling procedure was made by conducting FEM analysis of previously tested two wooden beams: solid wooden beam and FRP-strengthened wooden beam. Description of the modelling procedures for the two beams are described. Agreement between the numerically obtained and the experimentally observed flexural behaviour and failure validates the numerical modelling and analysis approach for investigating and design of various configurations for strengthening wooden elements. A numerical study was conducted to investigate several fiber composites strengthening schemes for wood beam.

Keywords: Wooden beams, strengthening, FRP, numerical modelling, finite elements, ABAQUS.

1. Introduction

Wood is one of the oldest building materials used throughout history. Wood has long been used as columns and as beams to support roofs due to its high strength in tension and compression in addition to its desirable properties of heat- sound-insulation. Long exposure of wooden elements over time to environmental conditions and misuse leads to damage and decay which necessitates restoration especially in case the building has historical and archaeological value. Different factors also lead to deterioration of the physical, chemical and mechanical properties of wood, and may finally lead to complete destruction; examples are exposure to acids, salts, sunlight and ultraviolet radiation, organisms, insects, termites and fungi [1].

Different restoration approaches may be applied for wooden roofs, such as removal of replacing damaged parts with new wood or adding a lightweight protection ceiling. Franke et al. [2] overviewed techniques for enhancing timber beam structural efficiency; these included substitution of wood with wood, mechanical fasteners and additional materials/products to increase strength limits. However, these methods violate the beauty and authenticity of the wooden roof. With the development in restoration methods, fiber- strengthened polymers (FRP) made of different fibers such as carbon, basalt, glass, etc. embedded in the polymer matrix are being used to restore wooden panels [3]. André and Kliger [4] presented a state-of-the-art review on research utilizing FRP to improve the mechanical properties of timber beams. Glass, carbon, and aramid fibers have been used to increase the flexural and/or shear capacity depending on the strengthening scheme. Different configurations can be used for applying FRP to wood surfaces using adhesives or mechanical fasteners, depending on the shape, size, and location of the reinforcement. Some common methods are shown in Figures 1-3. Wrapping can provide confinement and increase the load-carrying capacity of the wood. Figure 1 shows application of FRP sheets or strips on the outside of the wooden beams: glass, carbon or basalt FRP sheets or strips bonded to the tension side of the wood beams or side-bonding, U-shape or full-wrap [5, 6]. Rowlands et al. [7] proposed elaborating integrated glulam beams with GFRP embedded in the wood laminate. Borri et al. [8] provided wooden beams undersides and corners with FRP. Figure 2 shows FRP inserted in incisions. A technique involves slicing the specimen and inserting a plate in the cut. The plate must be secured with adhesive to the cross-section. Nowak et al. [9] inserted CFRP sheets in three lateral slits on each side. Kim et al [10] provided beams with an incision in the middle of the span and inserted different thicknesses of CFRP laminates. Jankowski et al. [11] investigated experimentally strengthening of 100-year-old wooden beams using CFRP strips. The results showed that CFRP is efficient for restoring and improving the load capacity of old deteriorated wooden beam, and concluded that the effectiveness of reinforcement depends on the quality of the wood-CFRP strip bond.

Figure 3 shows other configurations for FRP reinforcement of wooden beams. Osmannezhad et al. [12] proposed gluing GFRP between the layers. Shi et al. [13] glued GFRP into each joint and then around the perimeter of the beam cross-section. Raftery and Harte [14] used

GFRP to restore the mechanical strength and flexural stiffness of damaged glulam timber beams. Gand et al. [15] investigated the use of near-surface-mounted (NSM) FRP reinforcement as a viable option for strengthening timber structures. The average ultimate load capacity for FRP-strengthened beams was 16% higher than similar unstrengthened beams. The load-displacement curves showed a 30% rise in the stiffness of strengthened beams than that of unstrengthened beams.

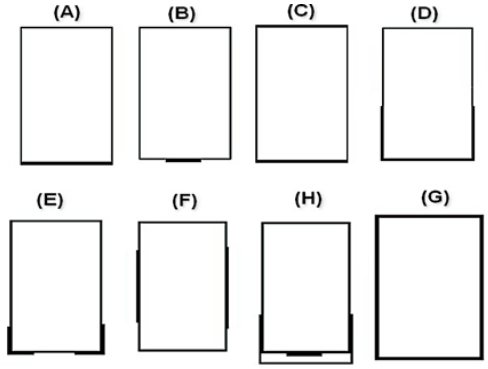

Fig. 1 Strengthening of wood beam sections by externally applied FRP

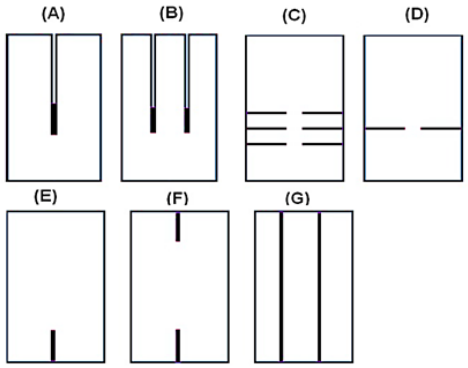

Fig. 2 Strengthening of wood beam sections by FRP applied internally or in incisions

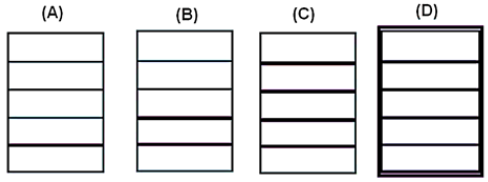

Fig. 3 Wooden beams strengthened by other configurations of FRP

Numerical modelling of timber beams is complicated due to the anisotropic nature of wood material, i.e. mechanical properties vary in the different directions, namely along grain and across grain; the problem is more complicated for FRP-strengthened wooden beams. Wood is also highly hygroscopic, i.e. easily acquires moisture, and may shrink transversally to the fibers forming cracks along the fibers, and thus reduce the shear resistance and the bearing capacity of wood [1]. The cycles of loss and absorption of water causes shrinkage and swelling which if not uniform causes warping, twisting, overstress and cracks [1]. Kim and Harries [16] simulated the behavior of timber beams strengthened with CFRP composites using 3D finite element using ANSYS analytical model, comparing numerical and experimental data, and conducting a parametric study to further study the effect of CFRP properties on wood species. Mascia et al. [17] developed a numerical modelling method of wooden beams strengthened with Vectran and glass fibres, which cost about 2.5 times less than carbon fibres, using computer software ANSYS v.12; that the fibres were shown to absorb a significant proportion of the acting stresses, decreasing the maximum values of the tensile stress and displacement. Kula and Socha [18] analysed wood beams strengthened with CFRP bands, using MES SIMULIA ABAQUS software and showed that strengthening with CFRP can decrease the rheological increases of deformation.

With the rising costs of experimental testing of full-scale wooden beams, and the need to keep up with the era of virtual reality to simulate restoration by creating a digital model that accurately reflects the laboratory and produces similar or matching results in many cases. The ABAQUS software was chosen to accomplish this research. Details of the steps to create the numerical model are presented, in addition to validation studies.

2. Numerical Modelling

Wood can be regarded as an orthotropic material, having independent mechanical properties in the directions of three mutually perpendicular axes: longitudinal axis L is parallel to the fiber (grain), radial axis R is normal to the growth rings (perpendicular to the grain in the radial direction), and tangential axis T perpendicular to the grain but tangent to the growth rings, as shown in Fig. 4. These axes determine behavior of wood under different types of stress and strain [1].

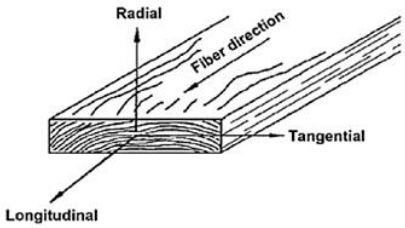

Fig. 4 The three principal axes of wood

In this work, numerical analysis is conducted by constructing a Finite Element Model (FEM) in ABAQUS, to simulate the mechanical behavior of wooden beams with fibre reinforcement inserted for enhancing flexural behaviour strength. The steps of this modelling process are described as follows.

- The first step involves importing 3D-CAD representations of the geometrical features of wood, fiber, and adhesive components.
- Definition of material properties of wood and fibres regarding modulus of elasticity and Poisson's ratio in three orthogonal directions. Hill criterion for material strength determinations in pertinent directions is employed [9, 19, 20]. Adhesive properties are delineated through use of cohesive elements [21]. The mechanical properties of wood and FRP given in Table 1 are drawn from experimental observations or literature references [1, 25].

- Establishment of constraints, interactions, and boundary conditions. In connecting assembly layers with other components, a TIE constraint is mandated, with the adhesive layer surfaces designated as the "slave" and the surfaces of the attached components as the "master." Rigorous attention is paid to articulating precise boundary conditions for the wood-fibre structure. For instance, a typical scenario involves fixing one end of the fibre and applying a load at the opposing end to simulate a tensile test.
- Generation of an appropriate mesh, with due consideration to the suggested stack direction.
- Configuration settings within ABAQUS are delineated. This involves defining the appropriate analysis type, usually static, and specification of additional parameters such as time period (set at 1) and the activation of Nlgeom to address nonlinearities. Throughout the analysis, automatic incrementation is employed with a small increment size, and the maximum number of increments is adjusted based on predefined criteria.
- Execution of the analysis itself, accompanied by diligent result monitoring to ensure conformity with anticipated behaviours. ABAQUS offers a suite of visualization tools, including contour plots and deformed shape renderings, to facilitate result interpretation and validation.

3. Verification Models

In order to ascertain the efficiency of the modelling procedure, comparative analysis was made between the outcomes and results obtained through experimental means. In case of disparities, adjustments were made to material properties or the model parameters, thus enhancing the model's precision. For validation, two models were made for wooden beams tested experimentally in two previously published researches [20, 21] illustrated in Figures 5 and 6. One of these models was a solid wooden beam, while the other incorporated fibre reinforcements.

Table 1 Mechanical properties of wood and FRP sheet

Parameter	Description	wood (Pine) start from-to	fiber sheet start from-to
E_1[MPa]	Elastic modules	8500-13500	38000-250000
E_2[MPa]		600-900	7000-18500
E_3 [MPa]		400-500	
v_{12}	Poisson ratios	0.33-0.335	0.2-0.35
v_{13}		0.33-0.358	
v_{23}		0.41-0.416	
G_{12} [MPa]	Shear modules	650-715	2730-7500
G_{13} [MPa]		529-650	
G_{23} [MPa]		69-100	
R_{11}	Hill criterion	0.484-1.2	1
$R_{22} = R_{33}$		0.061-0.9	0.025
$R_{12} = R_{13} = R_{23}$		0.206-0.67	0.016

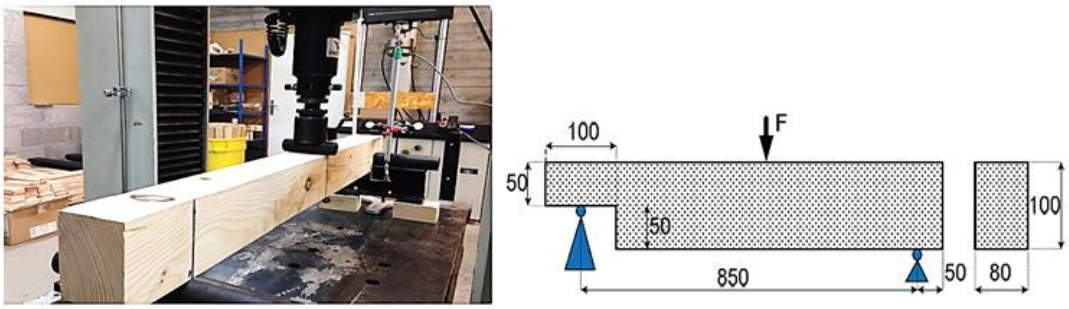

Fig. 5 Model I wooden beam (dimensions in mm) [20]

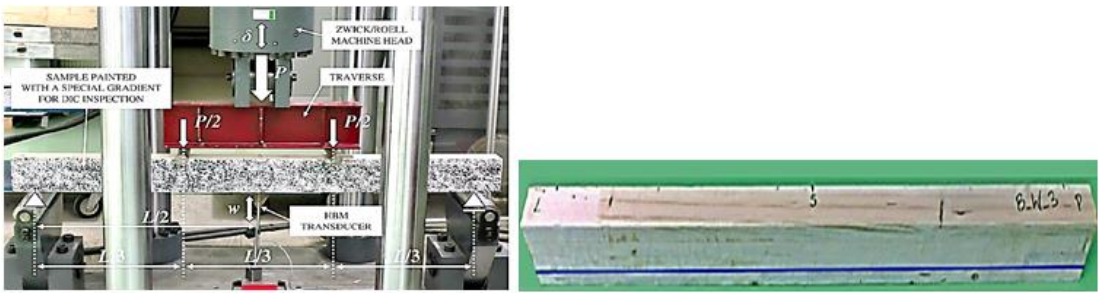

Fig. 6 Model II FRP-strengthened wooden beam [20]

3.1 Model Ⅰ: wooden beam

A three-dimensional numerical model was made for a solid beam previously tested by Tran et al. [20], having dimensions 900 x 100 x 80 mm, following the outlined steps. The created model employing 3D deformable/solid/extrusion format for wood, and for bottom steel plate 50 x 50 x 80 mm, the model was also in a 3D deformable/solid/extrusion format. Material attributes were configured encompassing Elastic Engineering Constants with values for E_1, E_2, E_3 (10000, 490, 490) MPa, Poisson Ratios ν_{12} , ν_{13}, ν_{23} (0.41, 0.41, 0.33) and shear moduli G_{12}, G_{13}, G_{23} (650, 650, 100) MPa, as derived from Table 1. Strength in the pertinent directions was determined through the utilization of the Hill criterion, integrating the Plastic Isotropic Adding Potential option with parameters R_{11}, R_{22}, R_{33}, R_{12}, R_{13}, R_{23} (0.48, 0.2, 0.2, 0.4, 0.4, 0.4), as given in Table 1. The assignment of material sections was executed as Solid/Homogeneous, with careful attention to align the wood component with the appropriate material orientation, as depicted in Figure 7. For inter-component connections, assembly layers were strictly constrained to interact solely via TIE constraints. Boundary conditions were defined for the wood, incorporating a displacement of -4.5 mm. Meshing was made for the wood and steel plate components, employing solid elements for wood (C3D8R), a general-purpose linear brick element, featuring 2x2x2 integration points, which was selected for its expedited computational efficiency compared to the general-purpose quadratic brick element C3D20R. Notably, Mesh/Orientation/Stack was integral to this process.

Numerical nonlinear analysis was executed using ABAQUS and results were shown through visualization tools as shown in Figs. 8 and 9. Comparison with laboratory results are given in Table 2 and plotted in Fig. 10. Notable agreement between the model-generated outcomes and laboratory results verifies the accuracy and reliability of the computational approach employed in the calculations, as shown by Table 2 and Figs 9 and 10.

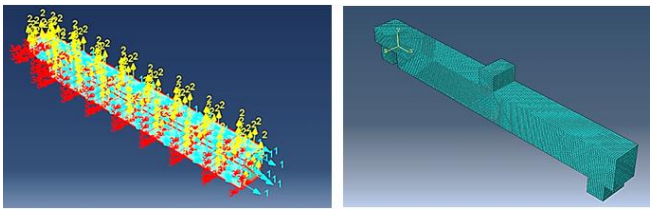

Fig. 7 Orientation of material axes and FEM mesh for Model I beam

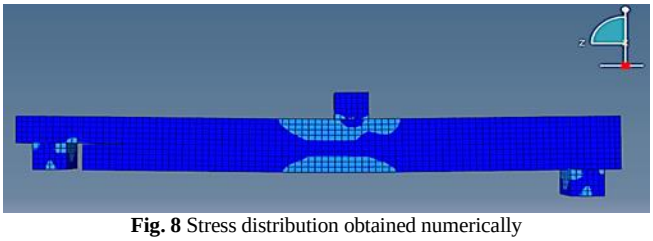

Fig. 8 Stress distribution obtained numerically

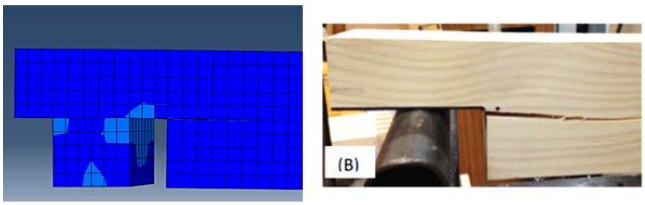

Fig. 9 Comparison between numerical crack and experimental crack

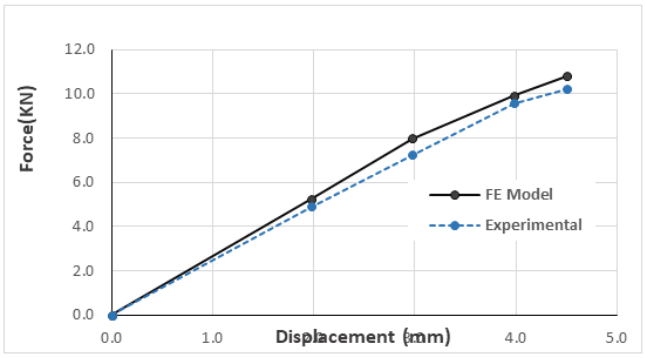

Fig. 10 Comparison between numerical and experimental load-deflection curve

Table 2 Comparison between numerical and experimental results

Mid-span deflection (mm)	Force (kN)	
	Numerical	Experimental
0.00	0.00	0.0
2.0	5.26	4.92
3.0	8.00	7.26
4.0	9.93	9.58
4.5	10.80	10.22

3.2 Model II fiber-strengthened wooden beam

A wooden beam measuring 93.5 x 39.75 x 2000 mm, adhesive layers with thickness of 0.1 mm and strengthened by CFRP layers 1.4 mm thick, the beam is supported on steel plates having dimensions 100 x 50 x 93.5 mm. The beam was tested experimentally by Kawecki and Podgórski [21]. Each of these components was represented in a 3D deformable/solid/extrusion format. Only half of the complete beam was modelled due to symmetry, as shown in Fig. 11.

Material properties were defined for both wood and CFRP, encompassing Elastic Engineering Constants, including elastic moduli (E_1, E_2, E_3), Poisson ratios (ν_{12} , ν_{13}, ν_{23}), and shear moduli (G_{12}, G_{13}, G_{23}), with the respective values detailed in Table 1. The modelling process also involved assessing strength in pertinent directions utilizing Hill criterion with parameters R_{11}, R_{22}, R_{33}, R_{12}, R_{13}, R_{23} specified in Table 3. Given the nature of laminated FRP composites and their susceptibility to interlaminar damage, special attention was dedicated to the properties of the

adhesive layers as shown in Fig.12. Elastic/Traction/Quads damage modelling was employed, assuming the characteristics of polyurethane (PUR) glue. Distinctions in stiffness and strength between wood-wood and wood-CFRP joints were accommodated as shown in Table 4 [21]. The choice of damage initiation criteria involved the application of a quadratic criterion, whereby damage initiation occurs when a specific combination of stress components surpasses a critical threshold. The Quads Damage option within the software facilitated the configuration of this criterion, with stress values, as outlined in Table 5, pertinent to wood-wood and wood-CFRP connections [22]. Additionally, the stress intensity factor for damage, described by Formula (1) [20].

$$\left(\frac{\sigma_n}{\sigma_n^c}\right)^2+\left(\frac{\sigma_s}{\sigma_s^c}\right)^2+\left(\frac{\sigma_t}{\sigma_t^c}\right)^2=1 \quad (1)$$

where, σ_n, σ_s ,σ_t based on the maximum stresses nominal stress and transversal directions as outlined in Table 5.

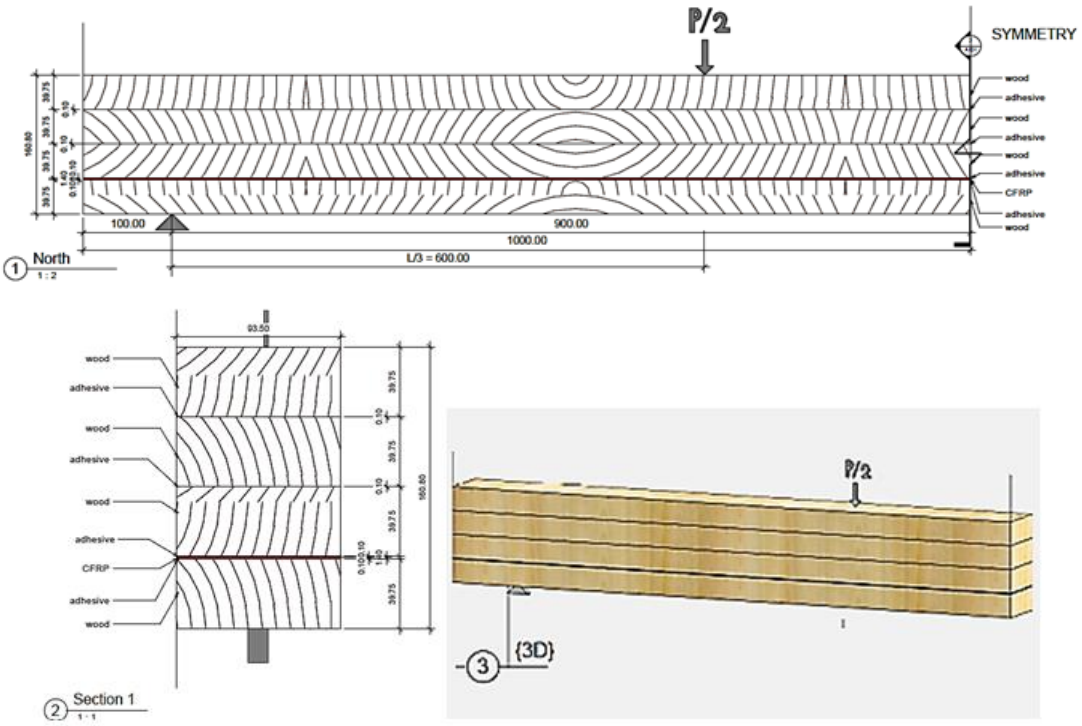

Fig. 11 Model II beam – beam cross-section and dimensions [21]

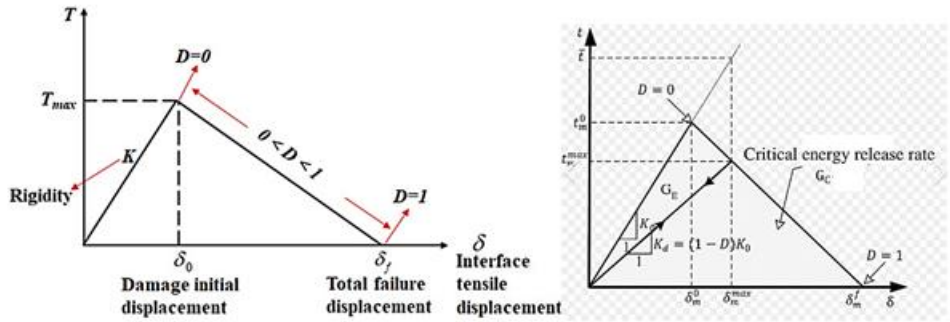

Fig. 12 Cohesive zone model and traction-separation law

Table 3 Material properties of wood and CFRP

Parameter	Wood (pine)	Fiber sheet
E_1 [Mpa]	11439	175000
E_2[Mpa]	732	7100
E_3 [Mpa]	458	
ν_{12}	0.335	0.3
ν_{13}	0.358	
ν_{23}	0.416	

Parameter	Wood (pine)	Fiber sheet
G_{13} [Mpa]	529	
G_{23} [Mpa]	69	
R_{11}	1.	1
$R_{22}=R_{33}$	0.065	0.025
$R_{12}=R_{13}=R_{23}$	0.25	0.016

Table4 Stiffness of wood-wood and stiffness of wood-CFRP

	E/Enn	G_1/Ess	G_2/Ett
Kww MPa/mm	91.32	91.32	91.32
Kwc MPa/mm	49.51	49.51	49.51

Table 5 Stress values

	Nominal stress (MPa)		
	Normal-only mode	first direction	second direction
Wood-wood	3.19	9.92	9.92
Wood-CFRP	2.23	6.94	6.94

Table 6 Values of energy

	Nominal stress (MPa)		
	Normal mode	Shear mode	
	Fracture energy	first -direction	second direction
Wood-wood	85.0	820	820
Wood-CFRP	42.0	402	402

Additionally, the stress intensity factor for damage was computed based on geometry, applied loads, and material properties. To model progressive delamination, BK energy and power values were set at 1.8, and corresponding energy release rates were defined for wood-wood and wood-CFRP connections [23, 24] as detailed in Table 6. To ensure stability of the model, a viscosity coefficient was introduced, with its value specified as 0.0005.

Material orientation was diligently managed, with wood benefiting from appropriate orientation techniques, while CFRP and adhesive components underwent reorientation via Tools/Datum and material orientation settings. Assigning material sections followed, with wood and steel plat sections designated as Solid/Homogeneous and CFRP configured as a composite layup for continuum shell modelling. The choice of continuum shell elements was made to enhance accuracy in contact modelling, particularly in scenarios involving large rotations and nonlinear geometric analyses. For the adhesive section, Other/Cohesive/Traction separation settings were employed, consistent with cohesive elements that enable comprehensive modelling of crack propagation problems, including crack initiation and propagation along predefined surfaces.

As with the first model, intercomponent connections were established exclusively through TIE constraints, maintaining the adhesive layer surfaces as "slaves" and the surfaces of attached components as "masters." Defining boundary conditions for the wood-fiber structure involved the application of a displacement of -28 mm, distributed across multiple steps to ensure precision.

Analysis considerations encompassed selecting an appropriate analysis type, typically static while defining parameters like a time period of 0.1 to expedite calculations. The activation of Nlgeom was crucial for accounting for nonlinearities, and an Automatic stabilization setting (Non) was chosen. Incrementation was automated, with the maximum number of increments increased by 10,000. Initial increment size, minimum increment, and maximum increment were set at 0.0001, 1E-015, and 0.1, respectively. A plane of symmetry (Symmetry/XSYMM) was also introduced, as illustrated in Fig. 13.

To enhance the accuracy and reliability of results, the iteration number was increased within Other/General Solution Controls/Manager settings.

Meshing was carried out for the CFRP-strengthened wooden beam, incorporating continuum shell elements for the CFRP (SC8R), solid elements for wood (C3D8), and cohesive elements for adhesive (COH3D8). A sufficiently fine mesh was made to precisely capture the behaviour of the wood-FRP system, with attention given to specifying stack directions for each component. Ultimately, the analysis was executed, and the results were systematically monitored using visualization tools of ABAQUS facilitating result interpretation shown in Fig. 13.

Comparison between the numerical and experimental outcomes revealed a striking convergence, with both sets of results exhibiting a remarkably close alignment. This close agreement is illustrated in Fig, 14, where the numerical data is graphically juxtaposed with the experimental findings. Furthermore, a quantitative examination of the results in

Table 7 underscores the remarkable proximity between the values obtained through numerical simulations and those derived from the physical experiments. These findings collectively attest to the robustness and accuracy of the numerical model, lending strong credence to its capacity for faithfully reproducing real-world behaviours.

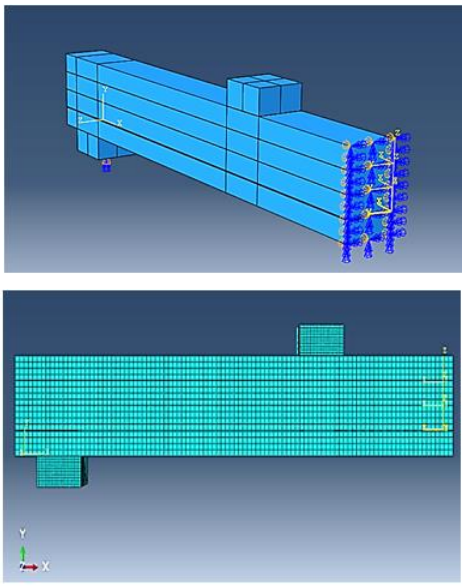

Fig. 13 FEM mesh for half of Model II beam

Table 7 Comparison between numerical and experimental results for model II

Mid-span deflection (mm)	Force (kN)	
	Numerical	Experimental
0	0	0
1.0	3.0	2.6
2.0	9.7	7.1
13.0	45.3	41.2
14.0	48.8	43.4
15.0	50.3	45.6
16.0	51.6	47.5
18.3	52.9	52.0
19.1	55.2	53.5
25.1	60.31	60.2

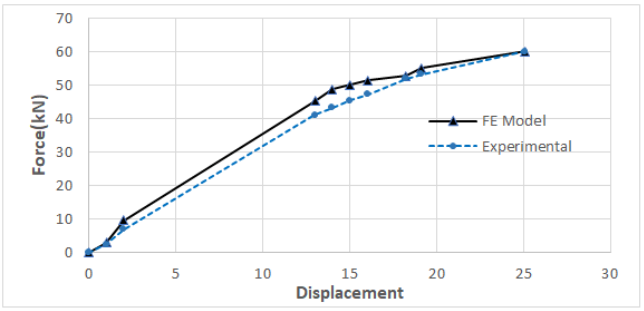

Fig. 14 Comparison between numerical and experimental load-deflection curve

4. Analytical Evaluation

The capacity of the wooden beam, Model I, is evaluated analytically using the bending strength values typical of this wood type and grade [1]. The characteristic value of bending strength is $f_{m,k}$ = 38 MPa

f_m=M/z

Z = (80*(100)^3)/ (12*(50)) = 133333.333 mm^3

M_m=Z * f =38*133333.333 =5066666.67 N.mm

M_m=P * L/4

P = 4 M_m/L=5066666.67x4/850 =23.843 kN

The material factor for structural timber, γ_m = 1.3, therefore

P = 23.84/1.3= 18.34 kN

This value is higher than the experimentally and numerically determined values 10.2 and 10.8 kN, respectively, which may be attributed to the non-homogeneity or defects present in the wooden beam, or also due to the nonlinear behaviour of wood.

5. Parametric Study

A parametric study was conducted where the first model of wood was strengthened with different fibers (Boron, Carbon, Glass, and Graphite), numerical modeling and nonlinear analysis was made as presented before. The numerical results are compared with the unstrengthened beam results in Table 8 and Fig. 15. The study demonstrates the capability of the adopted modeling procedure for representing the flexural behavior of wooden beams strengthened using various fiber materials.

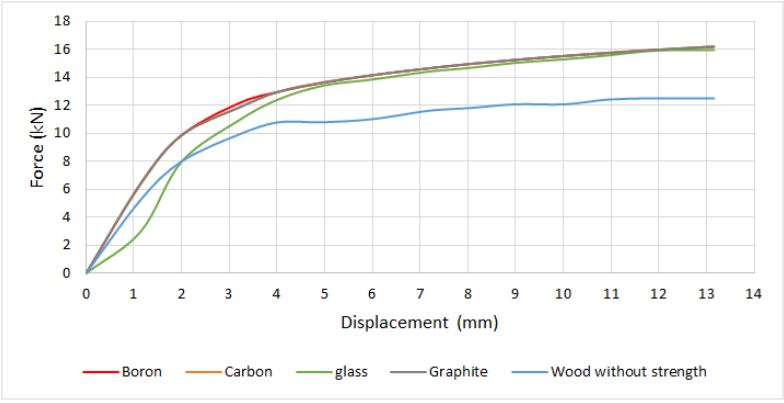

Fig. 15 Load-deflection curves for solid wooden beam and beam strengthened with different fibers

Table 8 Numerical study for different fiber reinforcements for wooden beam

Mid-span deflection (mm)	Force (kN) for unstrengthened wooden beam	Force (kN) for strengthened wood beams			
		Glass fibres	Boron fibers	Carbon fibers	Graphite fibers
0	0.00	0.0	0.0	0.0	0.0
1	5.26	3.0	6.4	6.4	6.4
2	8.00	8.0	9.9	9.9	9.9
3	9.93	10.9	12.2	11.8	11.9
4	10.80	12.4	13.0	13.0	13.0
5	10.80	13.4	13.6	13.7	13.6
6	11.02	13.8	14.2	14.2	14.2
7	11.62	14.4	14.7	14.7	14.7
8	11.82	14.7	15.0	15.0	15.0
9	12.08	15.0	15.3	15.3	15.3
10	12.08	15.3	15.5	15.6	15.5
11	12.43	15.6	15.8	15.8	15.8
12	12.51	15.9	16.0	16.0	16.0
13	12.5	16.0	16.2	16.2	16.2

6. Conclusions

In this paper numerical modelling was made using finite element method to investigate the flexural behaviour of wooden beams strengthened by FRP. NLFE model was made for two wooden beams that have been tested experimentally in published research, one solid beam and the other is a glulam beams fortified with FRP plates. The developed finite element models take into account the anisotropic nature and the nonlinear behaviour of wood and the orthotropic elasto-plastic properties of FRP, as well as the interface between FRP. The numerical results were discussed and compared with the published experimental results. The most significant conclusions from the research work are as follows.

1. Numerical modelling and analysis of the bending behaviour of both unstrengthened and FRP-strengthened wooden beams has been accomplished successfully.
2. The close alignment between the numerical results of load-deflection curves and their experimental counterparts demonstrates the model's capacity for accurately predicting the nonlinear behaviour of unstrengthen and strengthened timber beams.
3. The agreement observed between the numerical and experimental results for elastic stiffness, ultimate load, and mid-span deflection at failure further underscores the model's reliability and accuracy.
4. The model's adaptability extends to accommodating different loading combinations, geometric arrangements, or material characteristics, making it a valuable tool for refining the design of FRP-strengthened timber beams.
5. The proposed model can be applied for optimizing the design of timber beams strengthened with FRP composites. It readily adapts to various versatility loading scenarios, geometric configurations, and material attributes, offering a robust framework for design exploration.
6. Importantly, the suggested numerical model provides a cost-effective and time-efficient avenue for obtaining precise findings, minimizing the need for extensive and resource-intensive experimental trials.
7. This research has thus advanced the understanding of strengthened timber beam behaviour and also provided a powerful numerical tool that can facilitate the design and assessment of timber beams strengthened with FRP composites across a spectrum of real-world scenarios.

References

[1] Forest Products Laboratory, *Wood handbook: wood as an engineering material*, General Technical Report FPL-GTR-282. Madison, WI: U.S. Department of Agriculture, Forest Service, Forest Products Laboratory, 543 p., 2021

[2] S. Franke, B. Franke and A.M. Harte, "Failure modes and reinforcement techniques for timber beams – State of the art," *Constr Build Mater*, vol. 97, pp. 2–13, Oct. 2015, doi: 10.1016/j.conbuildmat.2015.06.021.

[3] F. H. Theakston, "A feasibility study for strengthening timber beams with fiberglass," *Can. Agric. Eng*, vol. 7, no. 1, pp. 17–19, 1965.

[4] A. André and R. Kliger, "Strengthening of timber beams using FRP with emphasis on compression strength: a state-of-the-art review", *Conference APFIS*, Seoul, Korea, 2009.

[5] P.R. Garcia, A. C. Escamilla and M.N.G. Garcia, "Analysis of the flexural stiffness of timber beams reinforced with carbon and basalt composite materials," *Compos B Eng*, vol. 86, pp. 152–159, 2016.

[6] J. Fiorelli and A. A. Dias, "Analysis of the strength and stiffness of timber beams reinforced with carbon fiber and glass fiber," *Mat Res*, vol. 6, no. 2, 193-202, 2003.

[7] R.E. Rowlands, R.P. Van Deweghe, T.L. Laufenberg, and G.P. Krueger, "Fiber-reinforced wood composites," *Wood and Fiber Science*, pp. 39–57, 1986.

[8] A. Borri, M. Corradi and A. Grazini, "FRP reinforcement of wood elements under bending loads", *Conference: Structural Faults and Repair*, London, 2003.

[9] T. P. Nowak, J. Jasieńko, and D. Czepizak, "Experimental tests and numerical analysis of historic bent timber elements

reinforced with CFRP strips," *Constr Build Mater*, vol. 40, pp. 197–206, 2013, doi: 10.1016/j.conbuildmat.2012.09.106.

[10] Y.J. Kim, M. Hossain, and K.A. Harries, "CFRP strengthening of timber beams recovered from a 32year old quonset: Element and system level tests," *Eng Struct*, vol. 57, pp. 213–221, 2013, doi: https://doi.org/10.1016/j.engstruct.2013.09.028.

[11] L.J. Jankowski, J. Jasieńko and T. P. Nowak, "Experimental assessment of CFRP reinforced wooden beams by 4-point bending tests and photoelastic coating technique," *Materials and Structures/Materiaux et Constructions*, vol. 43, no. 1–2, pp. 141–150, Jan. 2010, doi: 10.1617/s11527-009-9476-0.

[12] S. Osmannezhad, M. Faezipour and G. Ebrahimi, "Effects of GFRP on bending strength of glulam made of poplar (Populus deltoids) and beech (Fagus orientalis)," *Constr Build Mater*, vol. 51, pp. 34–39, 2014,

[13] H. Shi, W. Liu, H. Fang, Y. Bai and D. Hui, "Flexural responses and pseudo-ductile performance of lattice-web reinforced GFRP-wood sandwich beams," *Compos B Eng*, vol. 108, pp. 364–376, 2017.

[14] G.M. Raftery and A.M. Harte, "Repair of glulam beams using GFRP rods," in *WIT Transactions on the Built Environment*, 2009, pp. 417–427. doi: 10.2495/STR090371.

[15] A.K. Gand, D. Yeboah, M. Khorami, A.O. Olubanwo and R. Lumor, "Behaviour of strengthened timber beams using near surface mounted basalt fibre reinforced polymer (BFRP) rebars," *Engineering Solid Mechanics*, vol. 6, no. 4, pp. 341–352, 2018, doi: 10.5267/j.esm.2018.7.001.

[16] Y J. Kim and K.A. Harries, "Modeling of timber beams strengthened with various CFRP composites," *Eng Struct*, vol. 32, no. 10, pp. 3225–3234, Oct. 2010, doi: 10.1016/j.engstruct.2010.06.011.

[17] N.T. Mascia, C.A.A. Bertoline, C.D. Baságlia and B.F. Donadon, "Numerical analysis of glued laminated timber beams reinforced by Vectran fibers," *Ambiente Construído*, vol. 18, no. 3, pp. 359–373, Sep. 2018, doi: 10.1590/s1678-86212018000300286.

[18] K. Kula and T. Socha, "Renovation and strengthening of wooden beams with CFRP bands including the rheological effects," *Civil And Environmental Engineering Reports*, vol. 22, no. 3, pp. 93–102, Sep. 2016, doi: 10.1515/ceer-2016-0038.

[19] R. Hill, "A theory of the yielding and plastic flow of anisotropic metals," *Proc R Soc Lond A Math Phys Sci*, vol. 193, no. 1033, pp. 281–297, 1948.

[20] V.D. Tran, D. Dong and M. Oudjene, "Experimental and numerical analysis of the unreinforced and reinforced notched timber beam by a screw," *Vietnam Journal of Science, Technology and Engineering*, vol. 60, no. 3, pp. 26–32, Sep. 2018, doi: 10.31276/VJSTE.60(3).26.

[21] B. Kawecki and J. Podgórski, "The effect of glue cohesive stiffness on the elastic performance of bent wood–CFRP beams," *Materials*, vol. 13, no. 22, pp. 1–23, Nov. 2020, doi: 10.3390/ma13225075.

[22] A. Turon, C.G. Dávila, P.P. Camanho and J. Costa, "An engineering solution for mesh size effects in the simulation of delamination using cohesive zone models," *Eng Fract Mech*, vol. 74, no. 10, pp. 1665–1682, 2007,

[23] B. Kawecki, "Guidelines for FEM modelling of wood-CFRP beams using ABAQUS," *Archives of Civil Engineering*, vol. 67, no. 4, pp. 175–191, 2021, doi: 10.24425/ace.2021.138493.

[24] J. T. Wang, E.J. Pineda, V. Ranatunga and S.S. Smeltzer, "3D progressive damage modeling for laminated composite based on crack band theory and continuum damage mechanics," in *Annual Technical Conference of the American Society for Composites*, 2015.

[25] A. K. Kaw, *Mechanics of composite materials*. CRC press, 2005.